

Effect of Synthesizing Temperature on the Structure and Magnetic Properties of the Co-Ferrite

Zainab M. Kadhim, We'am S. Malik*

Department of Physics, College of Education, University of Al-Qadisiyah, Qadisiyah, Iraq.

*Corresponding author E-mail: weam.sami@qu.edu.iq

Doi: 10.29072/basjs.20230210

ARTICLE INFO	ABSTRACT
<p>Keywords</p> <p>Spinel ferrite; nanoparticles; magnetic properties; combustion; temperature.</p>	<p>This study explores the preparation of Co-nano ferrites using the glycine-nitrate auto-combustion method at different synthesis temperatures. The crystal structure, magnetic properties, and morphological traits were investigated using X-rays in diffractometry, a vibrating sample magnetometer, and scanning electron microscopy. Based on the X-ray diffraction (XRD) data, it can be observed that the products produced possess a cubic spinel structure. As the temperature for synthesis is elevated from 100°C to 250°C, there is an observed increase in the size of the crystallites from 21nm to 25nm. Furthermore, an increase in the synthesizing temperature led to a reduction in the lattice constant, which decreased from 8.4155 Å to 8.3565 Å. Scanning electron microscopy (SEM) images, accompanied by histograms, revealed that the ferrite nanoparticles exhibited a tendency to aggregate, as indicated by a variance of around 100 and a standard deviation of 10. The VSM data indicate that an increase in synthesis temperature leads to a corresponding increase in magnetic saturation.</p>

Received 3 July 2023; Received in revised form 12 Aug 2023, Accepted 26 Aug 2023, Published 31 Aug 2023



1. Introduction

In recent years, there has been a notable increase in the academic interest in synthesizing nanosized ferrites that exhibit magnetic properties significantly differing those observed in macroparticles of identical composition. This assertion is particularly applicable to the attributes exhibited by cobalt ferrite particles measuring around 10 nm in size [1]. These nanoparticles commonly exhibit unique characteristics that facilitate the exploration of novel applications. The physical and chemical properties of particles are greatly influenced by their composition, morphology, size, and shape. The enormous surface area of nanoparticles, which is a result of their small particle size, is an interesting feature [2]. Nanomaterials consist of atomic and molecular constituents with dimensions less than 0.2 nanometers. Nevertheless, block crystals that possess lattice spacing on the nanoscale scale yet exhibit macroscopic dimensions are typically excluded. The behavior of nanomaterials differs significantly from that of bulk materials primarily due to two factors: surface effects, which result in smooth scaling of properties due to the presence of atoms at the surface, and quantum effects, which manifest as discontinuous behavior resulting from the quantum confinement effect in materials with delocalized electrons. The mechanical, optical, electric, and magnetic properties of materials, as well as their chemical reactivity, are influenced by these variables [3]. Ferrite's magnetic properties can be largely determined by different elements, including crystal size, density, exchange interactions and anisotropy. Different magnetic properties, such as coercivity (H_c), remanence magnetization (M_r) and saturation magnetization (M_s) were recorded. It was found that the crystallite size and the value of M_s showed a positive association, which indicates that increasing the crystallite size can lead to an improvement in magnetization[4]. $CoFe_2O_4$ has a high coercivity, a medium saturation magnetization, and the highest magnetic crystallographic anisotropy. Additionally, it has high chemical and thermal stability, strong mechanical characteristics, and is also easy to manufacture using a variety of techniques [5, 4]. Cobalt ferrite nanoparticles have been prepared recently using a variety of methods, including ceramic processing [6], thermal decomposition method [7], Solvothermal method [8], One-pot hydrothermal and hydrothermal synthesis [9], micro-emulsion method [10], electrochemical method [11], sol-gel method [12]. The present investigation focuses on effect of the synthesizing temperature on the structure and magnetic properties of the Co-ferrite nanopowder by glycine-nitrate auto-combustion method at various temperatures and to analyze their structure, morphological and magnetic properties.



2. Materials and Method

The compounds $\text{Co}(\text{NO}_3)_2 \cdot 6\text{H}_2\text{O}$ and $\text{Fe}(\text{NO}_3)_3 \cdot 9\text{H}_2\text{O}$, obtained from Thomas Baker-India, were separately measured in terms of weight and subsequently dissolved in a predetermined quantity of water, maintaining a molar ratio of 1:2 for Co(II)/Fe(III). Glycine was introduced as a fuel into a nitrate solution at a mole ratio of 0.33. The mixture was agitated without the aid of a heat exchanger for a duration of 20 minutes, while maintaining an auto-combustion temperature of 100°C . Following the complete evaporation of the water, the gadget initiated the self-sustaining combustion process. The product underwent a triple cleaning process using ethanol and distilled water, followed by drying at a temperature of 75°C for one hour. In order to enhance the uniformity of the CoFe_2O_4 ferrites ash, the resulting products were subjected to grinding in a mortar for a duration of four minutes. The Co-ferrite was synthesized using the same techniques at preparation temperatures of 175°C and 250°C [24,25].

3- Characterization Techniques

A variety of characterization techniques, such as X-ray diffraction, vibrating sample magnetometer (VSM), and scanning electron microscopy (SEM), were employed to analyze the generated powders. The X-ray diffraction investigations were conducted using the Dx2700BH Multifunction x-ray diffract meter, which was produced in Japan. The device utilized a Cu target with a wavelength of 1.50 nm and covered a 2θ range from 10° to 80° . The morphology and elemental analyses of the sample were investigated using a scanning electron microscope, specifically the TESCN MIRA3 FRENCH. The experiments were conducted using an accelerated voltage of 10 kiloelectron volts (KeV). The experimental setup utilized in this study was a vibrating sample magnetometer (VSM) provided by MDK in Iran. The VSM was fitted with a magnet capable of generating a magnetic field strength of 1 Tesla. The measurements were conducted at room temperature.

4. Results and Discussion

4.1 Structural Analysis

Figure 1 illustrates the X-ray diffraction (XRD) patterns of CoFe_2O_4 samples synthesized at various temperature ranges. The Co-ferrite samples in their as-synthesized state revealed a cubic spinel structure, as evidenced by the diffraction peaks observed at (111), (220), (311), (222), (400), (422), (511), (440), and (620) planes. These diffraction peaks are consistent with the space group $\text{Fd}3\text{m}$. The X-ray diffraction (XRD) patterns were analyzed and verified using the Joint Committee



on Powder Diffraction Standards (JCPDS) database, with reference numbers 98-016-6204, 89-1010, and 22-1086, for the compound CoFe_2O_4 [23, 13]. The impurity phase of Fe_2O_3 ($2\theta = 36.35$ and 42.19) was seen in a sample synthesized at the synthesizing temperature of 100°C . As the synthesizing temperature rises, this impurity phase reduces.

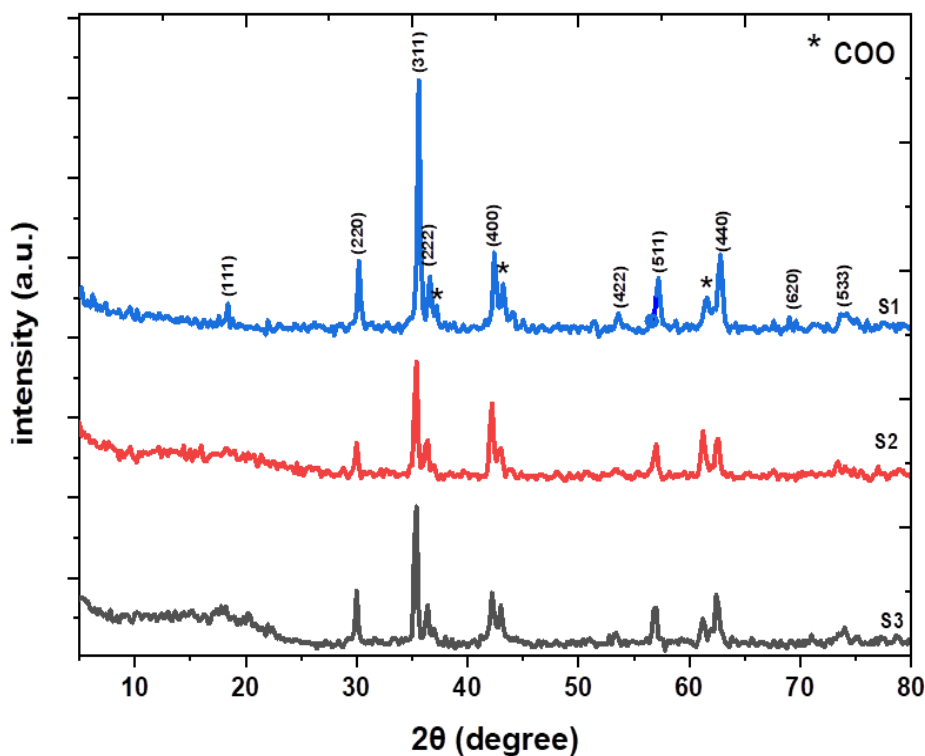


Figure1: XRD analyses of as-synthesized spinel CoFe_2O_4 powders at various synthesizing temperatures. (S1): 100°C , (S2): 175°C , and (S3): 250°C .

Also, the increase in synthesizing temperature leads to an increase in crystallite size, which produces narrow, sharp peaks that indicate the crystallinity of samples has been enhanced. The size of the crystallite and the lattice constant was calculated for CoFe_2O_4 samples depending on the equations below [14].

$$D = \frac{K\lambda}{\beta \cos\theta} \quad \text{----- (1)}$$

$$a = d_{hkl} \sqrt{h^2 + k^2 + l^2} \quad \text{----- (2)}$$

$$n \lambda = 2 d \sin \theta \quad \text{----- (3)}$$

In Debye Scherrer's equation (equ.1) K represents a constant equal to 0.89 is the dimensionless form parameter, the wavelength of X-rays is ($\lambda=1.5405 \text{ \AA}$), β is a representation of the diffraction line at half the maximum intensity of the high plane (311) and equ.2 represents Bragg's formula while equ.3 represents for finding the interplanetary spacing, where "h k l" are the Miller indices , " θ " is the Bragg diffraction angle , as well as "n = 1" for the cubic form's order of reflection and "a" for the lattice's constant.

Table 1: Crystallite size and lattice constant for Co-ferrite samples at various synthesizing temperatures.

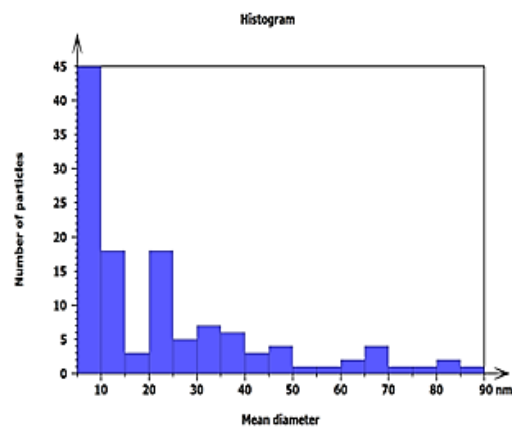
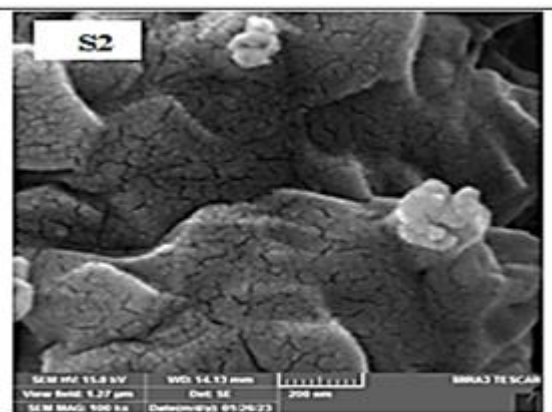
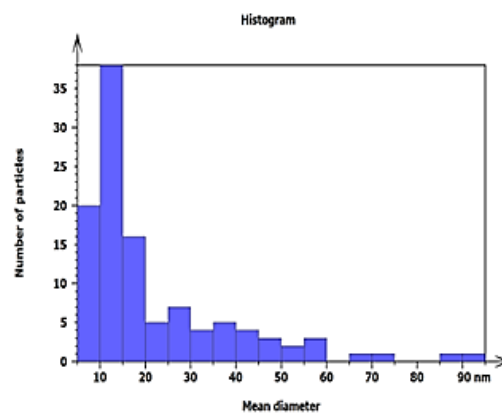
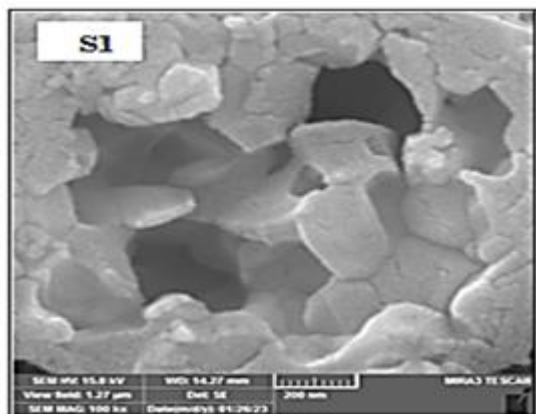
Synthesized Ferrites	T (°C)	2 θ (deg.)	Lattice Spacing d (Å)	Lattice Constant a (Å)	Crystallite Size D (nm)
S1	100	35.34	2.5374	8.4155	21
S2	175	35.36	2.5361	8.4112	22
S3	250	35.60	2.5196	8.3565	25

According to the data presented in Table 1, it is clear that as the synthesis's temperature increases from 100°C to 250°C, the crystallite size rises from 21nm to 25nm. Furthermore, increasing the synthesis temperature caused the lattice constant to decrease from 8.4155Å to 8.3565Å. According to the research, the lattice constant and crystallite size are directly connected. As crystallite size decreases, the lattice constant either rises or decrease [15]. In this work, as the size of the crystals increases, the lattice constant decreases. During synthesis, the fusion process, which takes place at high temperatures, may accelerate the rate of crystal size increase of the final product. D. Gingasu et al. observe the same observation [13].



4.2 Surface Morphology

The crystallite size of all synthesized Co-ferrite samples were calculated using the corresponding size distribution histograms. Figure 2(a–b) depicts SEM images and corresponding normal size distribution histograms by Origin 2021 software, and Figure 3 depicts EDAX spectra of CoFe_2O_4 spinel powders synthesized at different fabrication temperatures. (S1): 100°C, (S2): 175°C, and (S3): 250°C.



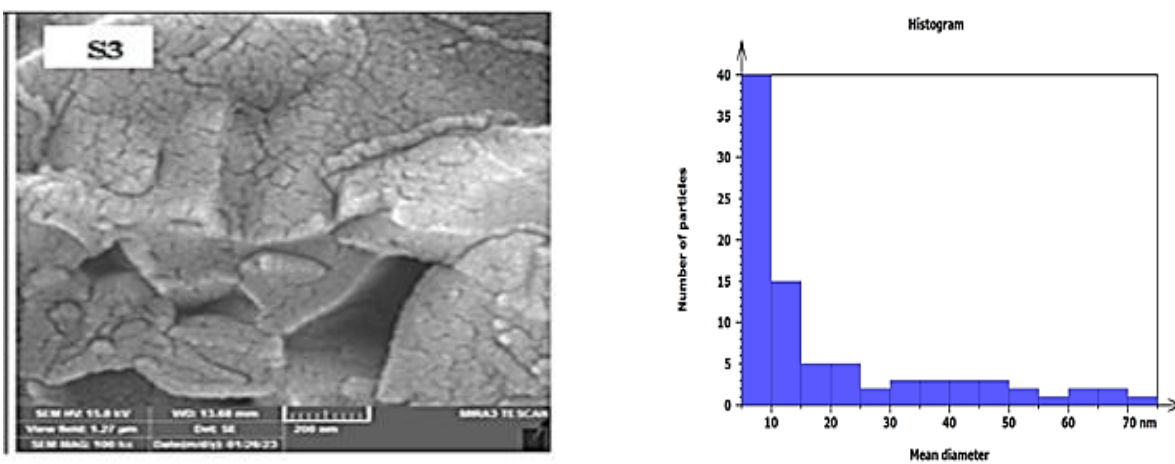


Fig.2 : SEM images (left, a) and (right, b) mean diameter histogram obtained from the SEM images of spinal CoFe_2O_4 ferrites powders produced by the glycine-nitrate auto-combustion method at various temperatures. (S1): 100°C , (S2): 175°C , and (S3): 250°C .

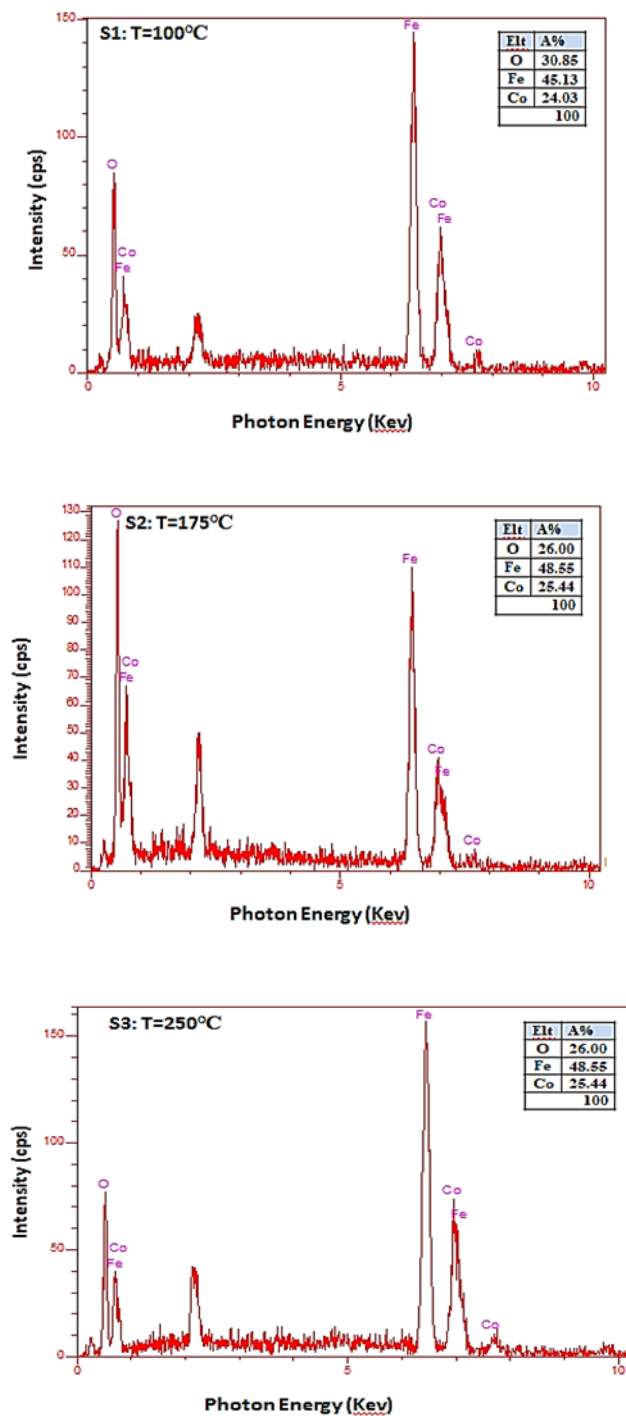


Fig.3: EDAX of spinal CoFe_2O_4 ferrites powders produced by the glycine-nitrate auto-combustion method at various temperatures (S1): 100°C, (S2): 175°C, and (S3): 250°C.

SEM images with histogram showed that all ferrite nanoparticles passes aggregated with variance and standard about 100 and 10 respectively. The structure of the aggregated nanopowder is shown in the adjacent SEM images and histograms. The results of the XRD examination were also supported by the observation that the crystalline size of the samples grew correspondingly with the synthesis temperature. When the nanoparticles' surface energy and surface area to the volume are ratio both very high, they clump together and expand into bigger assemblies as a treatment. The nanoscale particles have a tendency to aggregate in order to decrease the overall surface energy. The interaction of the magnetic nanoparticles may also contribute to agglomeration [16]. The impacts of the released gases from the combustion phase might cause a void in the powdered samples [17]. Co, Fe, and O are the fundamental compositional components of ferrites, according to an EDAX study of every Co-ferrite produced at various synthesis temperatures.

4.3 Magnetic Measurements

The magnetic behavior of CoFe_2O_4 powders with a spinel structure was investigated using the pulsed field hysteresis loop approach. The magnetization as a function of the applied field was determined for the ferrites under investigation at room temperature. This measurement was conducted at different synthesizing temperatures, and the applied field strength was set at 10 kilo-Oersteds (kOe). The obtained results are presented in Figure 4.

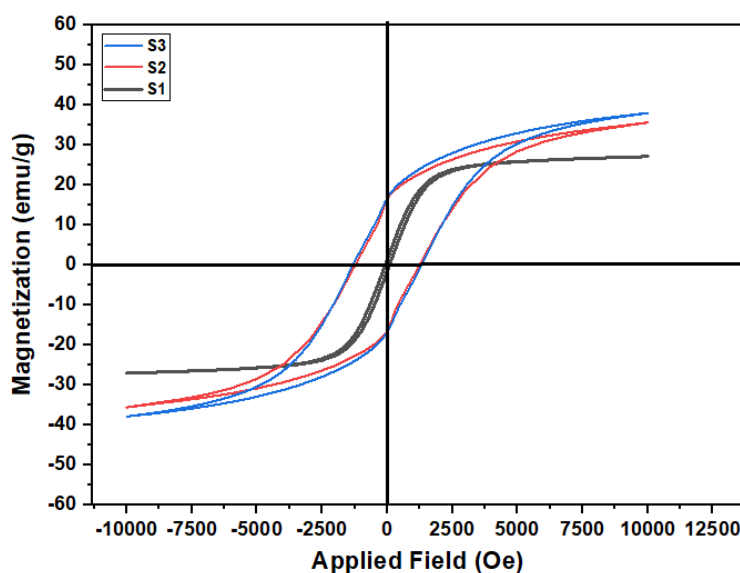


Fig.4: Magnetization versus applied field for as-synthesized spinel CoFe_2O_4 powders at various synthesizing temperatures. (S1): 100°C, (S2): 175°C, and (S3): 250°C.

The M-H plot displays a typical hysteresis curve, indicating that all spinel CoFe_2O_4 powders have ferromagnetic behavior. This M-H plot can be used to determine the saturation magnetization, remanence magnetization and coercivity of the present spinel CoFe_2O_4 powders. Table 2 lists the values of various magnetic properties.

Table 2: Magnetic measurements extracted of CoFe_2O_4 ferrite at different synthesizing temperatures.

Sample	Synthesizing Temperatures T (°C)	Saturation Magnetization Ms (emu/g)	Remanence Magnetization Mr (emu/g)	Coercivity Hc (Oe)	Mr/Ms
S1	100	27.06	5	125	0.1
S2	175	35.56	15	1000	0.4
S3	250	37.91	20	1125	0.5

From Table (2) It is clear that a rise in the synthesizing temperature gives an increase in saturation magnetization. The reason for this is attributed to this behavior for the saturation magnetization can be correlated to the presence of uncompensated spins at the surface of smaller particles. The high coercivity values account for the slower crystallite size growth rate that occurs during the heating phase. The increased coercivity value may be due to the direction of the magnetic spin along the axis that eases magnetization. The coercivity increases with the increase in saturation magnetization. Dedi et al. observe the same observation [18]. The squareness ratio (SQR) (M_r/M_s) for each sample has been calculated at RT which was less than 0.5 which means that one magnetic field sample was produced [19]. The magnetic properties of ferrite depend on the type of synthesis technique [20]. Different saturation magnetization values were reported and lasted in Table 3.



Table 3: Saturation magnetization of the as-synthesized spinel Co-ferrite powder with different methods.

Samples	Method	Applied field (Oe)	Ms	Ref.
CoFe ₂ O ₄	ceramic processing	7000	120	[6]
CoFe ₂ O ₄	glycine-nitrate process	15000	70	[21]
CoFe ₂ O ₄	Co-precipitation	15000	30	[22]
CoFe ₂ O ₄	glycine-nitrate auto-combustion process	10000	35.56	Present work

5. Conclusions

In the current study, Co-ferrite has been successfully prepared by the glycine nitrate auto-composition process. This process is simple and easy and suitable for synthesized spinel ferrite with small crystallite size. In the present work, Co-ferrite nanoparticles with crystallite size from 21nm to 25nm were produced. SEM images with histogram showed that all ferrite nanoparticles pass aggregated with variance and standard about 100 and 10 respectively. Magnetic measurements depended on the synthesizing temperature, as rising synthesizing temperature gives an increase in magnetic saturation.

Acknowledgments

The Al-Qadesiya University, Iraq, Najaf Examination Center, Najaf, Iraq; Anwar Al-Razi's service laboratory of the Baghdad Company, Iraq; Mashhad University, Mashhad, Iran for providing characterizations facilities for the current work; and Kashan University, Kashan, Iran are all acknowledged by the authors.



References

- [1] V.A. Kuznetsova, O.V. Almjasheva, V.V. Gusarov, Influence of Microwave and Ultrasonic Treatment on The Formation of CoFe_2O_4 Under Hydrothermal Conditions, *Glass Phys. Chem.*, 35(2009)205–209, [Doi:10.1134/S1087659609020138138](https://doi.org/10.1134/S1087659609020138138)
- [2] O.K. Mmesles, N. Masunga, A. Kuvarega, T. TI. Nkambule, B.B. Mamba, K. K. Kefeni, Cobalt Ferrite Nanoparticles and Nanocomposites: Photocatalytic, Antimicrobial Activity and Toxicity in Water Treatment, *Mater. Sci. in Semi. Pro.*, 123, (2021), 105523, <https://doi.org/10.1016/j.mssp.2020.105523>
- [3] C. Buzea, I.I. Pacheco, K. Robbie, Nanomaterials and Nanoparticles: Sources and Toxicity, *Biointerphases*, 2 (2007)17-71, <https://doi.org/10.1116/1.2815690>
- [4] N. T. T. Loan, N. T. H. Lan, N. T. T. Hang, N. Q. Hai, D. T. T. Anh, V. T. Hau, L. V. Tan, T. V. Tran, CoFe_2O_4 Nanomaterials: Effect of Annealing Temperature on Characterization, Magnetic, Photocatalytic, and Photo-Fenton Properties, *Processes*, 7(2019) 885, <https://doi.org/10.3390/pr7120885>
- [5] V. Mameli, A. Musinu, A. Ardu, G. Ennas, D. Peddis, D. Niznansky, C. Sangregorio, C. Innocenti, N.T. K. Thanh, C. Cannas, Studying the effect of Zn-substitution on the magnetic and hyperthermic properties of cobalt ferrite nanoparticles, *Nanoscale*, 8 (2016) 10124–10137, [10.1039/C6NR01303A](https://doi.org/10.1039/C6NR01303A)
- [6] A. Hassadee, T. Jutarosaga, W. Onreabroy, Effect of zinc substitution on structural and magnetic properties of cobalt ferrite, *Procedia Eng.*, 32 (2012) 597 – 602, <https://doi.org/10.1016/j.proeng.2012.01.1314>
- [7] W. Kachi, A.M. AL-Shammari, I.G. Zainal, Cobalt Ferrite Nanoparticles: Preparation, characterization and salinized with 3-aminopropyl triethoxysilane, *Energy Procedia*, 157 (2019) 1353–1365, [doi:10.1016/j.egypro.2018.11.300](https://doi.org/10.1016/j.egypro.2018.11.300)
- [8] A. Kalam, A.G. Al-Sehemi, M. Assiri, G. Du, T. Ahmad, I. Ahmad, M. Pannipara, Modified Solvothermal Synthesis of Cobalt Ferrite (CoFe_2O_4) Magnetic Nanoparticles Photocatalysts for Degradation of Methylene Blue with H_2O_2 /Visible Light, *Results Phys.*, 8 (2018) 1046–1053, <https://doi.org/10.1016/j.rinp.2018.01.045>
- [9] N. M. Refat, M. Y. Nassar, S. A. Sadeek, A controllable one-pot hydrothermal synthesis of spherical cobalt ferrite nanoparticles: synthesis, characterization, and optical properties, *RSC Adv.*, 12(2022)25081–25095, <https://doi.org/10.1039/D2RA03345C>



- [10] M. Ristić, S. Krehula, M. Reissner, M. Jean, B. Hannoyer, S. Musić, "Synthesis and Properties of Precipitated Cobalt Ferrite Nanoparticles" *J. Mol. Str*, 1140(2017) 32-38, <https://doi.org/10.1016/j.molstruc.2016.09.067>
- [11] M. Kooti, M. Afshari, Magnetic Cobalt Ferrite Nanoparticles as an Efficient Catalyst for Oxidation of Alkenes, *Scientia Iranica*, 19(2012)1991–1995, <https://doi.org/10.1016/j.scient.2012.05.005>
- [12] N. Abbas, N. Rubab, N. Sadiq, S. Manzoor, M. I. Khan, J. F. Garcia, I. B. Aragao, M. Tariq, Z. Akhtar, G. Yasmin, Aluminum-Doped Cobalt Ferrite as an Efficient Photocatalyst for the Abatement of Methylene Blue, *Water J.*, 12 (2020) 2285, <https://doi.org/10.3390/w12082285>
- [13] D. Gingasu, L. Diamandescu, I. Mindru, G. Marinescu, D.C. Culita, J.M. Calderon-Moreno, I. S. Preda, C. Bartha, L. Patron, "Chromium Substituted Cobalt Ferrites by Glycine-Nitrates Process, *Croat. Chem. Acta*, 88(2015) 445–451, <https://doi.org/10.5562/cca2743>
- [14] W.A. Farooq, M.S. Ul Hasan, M.I. Khan, A.R. Ashraf, M.A. Qayyum, N. Yaqub, M.A. Almutairi, M. Atif, A. Hanif, Structural, Optical and Electrical Properties of $\text{Cu}_{0.6}\text{Co}_x\text{Zn}_{0.4-x}\text{Fe}_2\text{O}_4$ ($x = 0.0, 0.1, 0.2, 0.3, 0.4$) Soft Ferrites, *Molecules*, 26(2021)1-10, <https://doi.org/10.3390/molecules26051399>
- [15] L.R. Nivedita, A. Haubert, A.K. Battu, C.V. Ramana, Correlation Between Crystal Structure, Surface/Interface Microstructure, and Electrical Properties of Nanocrystalline Niobium Thin Films, *J. Nanomater.*, 10(2020)1-23, <https://doi.org/10.3390/nano10071287>
- [16] D. Guragain, B.K. Rai, S. Yoon, T.P. Poudel, S.Ch. Bhandari, S.R. Mishra, Effect of Terbium Ion Substitution in Inverse Spinel Nickel Ferrite: Structural and Magnetic Study, *J. Magnetochemistry*, 6(2020)1-9, <https://doi.org/10.3390/magnetochemistry6010014>
- [17] R. Sepahvandi, H. Masoudi, E. Khosravi, B. Nayebi, Structural and Magnetic Properties of $\text{Co}_{1-x}\text{Mg}_x\text{Fe}_2\text{O}_4$ Nanoparticles Synthesized by Microwave-Assisted Combustion Method, *J Supercond Nov Magn*, 30 (2017) 1801–1805, DOI:[10.1007/S10948-017-3974-Z](https://doi.org/10.1007/S10948-017-3974-Z)



- [18] D. N. Idayanti, T. Kristiantoro, G.F.N. Alam, N. Sudrajat, Magnetic properties of cobalt ferrite synthesized by mechanical alloying, *J. AIP Advances*, 1964(2018) 020003, <https://doi.org/10.1063/1.5038285>
- [19] M.A. Almessiere, Y. Slimani, M. Sertko, M. Nawaz, A. Sadaqat, A. Baykal, I. Ercan and B. Ozcelik, Effect of Nb³⁺ Substitution on the Structural, Magnetic, and Optical Properties of Co_{0.5}Ni_{0.5}Fe₂O₄ Nanoparticles, *J. Nanomaterials*, 9 (2019) 430, <https://doi.org/10.3390/nano9030430>
- [20] T. Anjaneyulu, A.T Raghavender, K.V Kumar, P.N Narayana, K. Narendra, Effect of Crystallite size on the Structural and Magnetic Properties of, Nanocrystalline Zinc Ferrite, *Sci. Technol. Arts Res. J.*, 3(2014)48-51, DOI: <http://dx.doi.org/10.4314/star.v3i3.8>
- [21] K.L. Routray, D. Sanyal, D. Behera, Dielectric, Magnetic, Ferroelectric, and Mossbauer Properties of Bismuth Substituted Nanosized Cobalt Ferrites Through Glycine Nitrate Synthesis Method, *J. Appl. Phys.* 122(2017) 224104, <https://doi.org/10.1063/1.5005169>
- [22] S. Dabagh, K. Chaudhary, Z. Haider, J. Ali, Study of Structural Phase Transformation and Hysteresis Behavior of Inverse-Spinel α -Ferrite Nanoparticles Synthesized by Coprecipitation Method", *J. Results Phys*, 8(2018)93-98, <https://doi.org/10.1016/j.rinp.2017.11.033>
- [23] S. Iqba, M. F. Alam, M. Atif, N. Amin, K.S. Alimgeer, A. Ali, A. Ahmad, A. Hanif, W. A. Farooq, Structural, Morphological, Antimicrobial, and in Vitro Photodynamic Therapeutic Assessments of Novel Zn⁺²-Substituted Cobalt Ferrite Nanoparticles, *J. Results Phys*, 15(2019)102529, <https://doi.org/10.1016/j.rinp.2019.102529>
- [24] W. Sami, The Effect of Temperature on The Physical and Magnetic Properties of Ni-Ferrite Powder Preparation, *J. AIP Conf. Proc.*, 2845(2023) 070028, <https://doi.org/10.1063/5.0157328>
- [25] W. Sami, Synthesis and Study of Temperature Effect on The Spectroscopic Properties of The Nickel Ferrites by Glycine-Nitrate Auto-Combustion", *Bas J Sci*, 40 (2022)138-149, [Doi:10.29072/basjs.20220108](https://doi.org/10.29072/basjs.20220108)



تأثير درجة حرارة التصنيع على الخواص التركيبية والمغناطيسية لفرايت الكوبلت

زينب محمد كاظم ، ونام سامي مالك

جامعة القادسية – كلية التربية – قسم الفيزياء

المستخلص :

في هذا العمل تم دراسة تركيب الفرايت النانوي بطريقة الاحتراق التلقائي للجليسين- نترات عند درجات حرارة تصنيع مختلفة , بواسطة الأشعة السينية المستخدمة لمقياس الحيود ، مقياس المغناطيسية للعينة الاهتزازية والمسح المجهر الإلكتروني . تمت دراسة التركيب البلوري والخصائص المغناطيسية و الشكلية. وفقاً لبيانات XRD ، فإن المنتجات المركبة لها هيكل إسبينل مكعب . نظراً لارتفاع درجة حرارة التركيب من 100 درجة مئوية إلى 250 درجة مئوية ، يزداد حجم البلورات من 21 نانومتر إلى 25 نانومتر. بالإضافة إلى ذلك ، أدى ارتفاع درجة حرارة التركيب إلى انخفاض ثابت الشبكة من 8.4155 أنكستروم إلى 8.3565 أنكستروم . أظهرت صور SEM مع الرسم البياني أن جميع الجسيمات النانوية الفرايتية تمر متكتلة بتباين ومعياري حوالي 100 و 10 على التوالي. اعتماداً على قياسات VSM ، وجد أن ارتفاع درجة حرارة التركيب يعطي زيادة في التشبع المغناطيسي.